Research Article

Elham Alali and Ahmed M. Megahed*

MHD dissipative Casson nanofluid liquid film flow due to an unsteady stretching sheet with radiation influence and slip velocity phenomenon

https://doi.org/10.1515/ntrev-2022-0031
received October 30, 2021; accepted January 3, 2022

Abstract: The problem of non-Newtonian Casson thin film flow of an electrically conducting fluid on a horizontal elastic sheet was studied using suitable dimensionless transformations on equations representing the problem. The thin film flow and heat mechanism coupled with mass transfer characteristics are basically governed by the slip velocity, magnetic field, and the dissipation phenomenon. The present numerical analysis by the shooting method was carried out to study the detailed, fully developed heat and mass transfer techniques in the laminar thin film layer by solving the competent controlling equations with eight dominant parameters for the thin liquid film. Additionally, the predicted drag force *via* skin-friction coefficient and Nusselt and Sherwood numbers were correlated. In view of the present study, a smaller magnetic parameter or a smaller slip velocity parameter exerts very good influence on the development of the liquid film thickness for the non-Newtonian Casson model. Furthermore, a boost in the parameter of unsteadiness causes an increase in both velocity distribution and concentration distribution in thin film layer while an increase in the same parameter causes a reduction in the film thickness. Likewise, the present results are observed to be in an excellent agreement with those offered previously by other authors. Finally, some of the physical parameters in this study, which can serve as improvement factors for heat mass transfer and thermophysical characteristics, make nanofluids premium candidates for important future engineering applications.

Keywords: nanofluid Casson thin film, unsteady stretching sheet, viscous dissipation, thermal radiation, slip velocity, Joule heating

1 Introduction

The mechanism of heat transfer occurring through a thin liquid film past an elastic sheet is given further attention, because it has enormous applications in industry, many technology fields and engineering disciplines. Typical applications include foodstuff processing reactor fluidization, polymer processing, fiber coating, and solar cell encapsulation. In recent years, due to the immense importance of this field, the rheological physical properties of thin films have attracted the attention of many researchers. Wang [1] pioneered a rare exact solution for unsteady fluid film flow problems and heat transfer properties regarding an accelerating elastic sheet. His novel similarity transformations were found to fulfill the full equations of Navier–Stokes together with the equations of the boundary layer. Thus, the study of the topic of flow of liquid thin film together with the mechanism of heat transfer past a flexible sheet has been the leading topic of a huge number of scientific projects in the past [2–5]. Later on, Chen [6] took into account the Marangoni impact and forced and mixed convection phenomenon on the problem which investigate the flow of the fluid and heat transfer within a non-Newtonian power-law thin film due to stretched surface. Liu and Andersson [7] examined the fluid flow problem together with the heat transfer process which occur in the thin liquid film layer which is forced by a flexible sheet surface with variable stretching rate and variable surface temperature. Recently, Abel *et al.* [8], Noor *et al.* [9], Noor and Hashim [10], Nandeppanavar *et al.* [11], Liu and Megahed [12], and Khader and Megahed [13] have examined the heat transfer mechanism through a liquid thin film due to an unsteady stretching sheet for different physical assumptions such as viscous dissipation, thermocapillarity phenomenon, thermal

* **Corresponding author: Ahmed M. Megahed,** Department of Mathematics, Faculty of Science, Benha University, Benha, Egypt, e-mail: ahmed.abdelbaqk@fsc.bu.edu.eg
Elham Alali: Department of Mathematics, Faculty of Science, University of Tabuk, Tabuk 71491, Saudi Arabia, e-mail: Eal-ali@ut.edu.sa

radiation, internal heat generation, and external magnetic field. Among the previous non-Newtonian studied problems, the non-Newtonian Casson model has received more attention. Casson fluid has distinct characteristics in which it can treat fluids which have an infinite viscosity at the absence of the shear rate. This type of fluid is usually essential in bioengineering activities, food manufacturing, and some of the important metallurgical processes [14–16].

Nowadays, nanotechnology is an attractive area of research due to its wide use in traditional industry and technological applications such as polymers, insulating materials, and heat exchange media. Nanoparticles are distinguished by nanometer cereal sizes which possess unrivaled electrical and chemical characteristics. A formidable advantage of this novel scientific field is that nanomaterials can be scattered in fluids, especially the traditional heat transfer fluids [17]. For more detailed information on the topic of nanofluid science and historical aspects of the enhancement mechanism of convective heat transfer, we refer to the paper by Kakaç and Pramuanjaroenkij [18]. As pointed out by Khan and Pop [19], the thermal conductivity of some fluids can be improved by hanging micro (nano) material particles in fluids. Also, they reported that the heat transfer mechanism can be improved by adding microscale particles to the principle fluid. The potential mechanism of heat generation or absorption properties on the nanofluid flow and heat transfer through saturated porous media was examined by Hamad and Pop [20]. On the other hand, they considered that the field of nanofluid technology is one of the serious sciences that may control the next senior technological revolution of this century. The highest precision of the manufacturing product in the microfluid flow due to a heated porous elastic sheet process can be obtained by accurate control of flow and heat transfer [21,22]. Very recent studies on the topic of nanofluid flow and heat transfer with different important physical assumptions can be consulted in refs [23–26].

Based on the research above and motivated by the possible technological applications regarding the nanofluid issues of non-Newtonian Casson fluids due to the flexible sheet, the purpose of the present work is to present a numerical solution for the physical problem which describes the simultaneous fluid flow mechanism and heat mass transfer properties of a laminar thin film layer of an electrically conducting non-Newtonian Casson nanofluid subject to an unsteady elastic sheet with radiation mechanism, viscous dissipation phenomenon, and slip velocity. The findings of this theoretical scientific project are presumed to be helpful to the thermo community in the field of nanofluid flow, especially in the cooling process efficiency through some future industrial techniques.

2 Formulation of the problem

First, we must recall the definition of nanofluids from the literature review. The heat transfer liquids that are newly used in more technological applications are nanofluids. This important type of fluid is advanced by hanging micro-sized solid particles in the base fluid. Due to the chaos movement of the hanging particles in a liquid, this motion is described by a Brownian motion with a Brownian diffusion coefficient D_B. Also, in nanofluid movement, there is a distinct response for the suspended particles to the temperature gradient, which can be observed in the form of a thermophoretic phenomenon with a thermophoretic diffusion coefficient D_T. Here, we assume an electrically conducting, radiative non-Newtonian Casson nanofluid flow, which is characterized by β parameter due to an unsteady elastic sheet simultaneously with the impact of the magnetic field and including the influence of chemical reaction. Additionally, the proposed magnetic field is assumed to depend nonlinearly on the time according to the following relation:

$$B(t) = \frac{B_0}{\sqrt{1 - at}}, \tag{1}$$

clearly that at $t = 0$ the magnetic field strength $B(t)$ becomes equal to B_0 and a is a constant with dimension $\frac{1}{t}$. Likewise, the influences of Brownian motion, slip velocity phenomenon, and thermophoresis through a sheet are also considered. Further, all physical properties are assumed to be constants. By recalling all of the Boussinesq and Rosseland diffusion approximations, the governing equations for our physical investigation can be written as [27]:

$$\frac{\partial u}{\partial x} + \frac{\partial v}{\partial y} = 0, \tag{2}$$

$$\frac{\partial u}{\partial t} + u\frac{\partial u}{\partial x} + v\frac{\partial u}{\partial y} = \nu\left(1 + \frac{1}{\beta}\right)\frac{\partial^2 u}{\partial y^2} - \frac{\sigma B^2}{\rho_f}u, \tag{3}$$

$$\begin{aligned}\frac{\partial T}{\partial t} + u\frac{\partial T}{\partial x} + v\frac{\partial T}{\partial y} &= \alpha\frac{\partial^2 T}{\partial y^2} + \frac{\nu}{c_p}\left(1 + \frac{1}{\beta}\right)\left(\frac{\partial u}{\partial y}\right)^2 + \frac{\sigma B^2}{\rho_f c_p}u^2 \\ &\quad - \frac{1}{\rho_f c_p}\frac{\partial q_r}{\partial y} + \tau\left(D_B\left(\frac{\partial C}{\partial y}\frac{\partial T}{\partial y}\right) + \left(\frac{D_T}{T_0}\right)\left(\frac{\partial T}{\partial y}\right)^2\right),\end{aligned} \tag{4}$$

$$\frac{\partial C}{\partial t} + u\frac{\partial C}{\partial x} + v\frac{\partial C}{\partial y} = D_B\frac{\partial^2 C}{\partial y^2} + \left(\frac{D_T}{T_0}\right)\frac{\partial^2 T}{\partial y^2}. \tag{5}$$

In the overhead equations, u and v are the nanofluid velocity components. Moreover, the symbols α and ρ_f represent the fundamental fluid thermal diffusivity and the density of the Casson nanofluid, respectively. Another property for the present physical problem is the ratio of the microparticle heat capacity to the fundamental fluid heat capacity, which is mathematically symbolized by τ. Also, the nanofluid electric conductivity is measured by σ and the nanofluid kinematic viscosity is denoted by ν. Furthermore, from the aforementioned equations we observe a robust coupling between the nanofluid temperature T and the nanoparticle volume fraction C. Here, we must refer to the fact that the present non-Newtonian Casson model is valid for all values of β greater than zero. Also, we must mention that when $\beta \to 0$ our model reduces to the Newtonian model. Finally, q_r which is basically associated with the energy equation denotes the radiative heat flux and it is further defined and simplified linearly previously by everyone who studied the thermal radiation phenomenon, see for example, Raptis [28,29]. The proposed nanofluid is incompressible and hence the boundary conditions can undergo the following equations:

$$\begin{aligned} &u = U + N_1\left(1 + \frac{1}{\beta}\right)\frac{\partial u}{\partial y},\ v = 0,\\ &T_w = T_0 - T_r\left(\frac{bx^2}{2\nu}\right)(1 - at)^{\frac{-3}{2}},\\ &C_w = C_0 - C_r\left(\frac{bx^2}{2\nu}\right)(1 - at)^{\frac{-3}{2}},\ \text{at } y = 0, \end{aligned} \tag{6}$$

$$\begin{aligned} &\left(\frac{\partial u}{\partial y}\right)_{y=h} = 0,\ \left(\frac{\partial T}{\partial y}\right)_{y=h} = 0,\ \left(\frac{\partial C}{\partial y}\right)_{y=h} = 0,\\ &(v)_{y=h} = \frac{\mathrm{d}h}{\mathrm{d}t}, \end{aligned} \tag{7}$$

where T_w is the sheet temperature, T_0 is the fluid temperature at the slot, T_r is the constant reference temperature, C_0 is the fluid concentration at the slot, C_w is the nanoparticle volume fraction, and C_r is the constant reference nanoparticle volume fraction. The physical meaning which can be concluded here from the first portion of equation (6) is that our model is basically based on the fact of the slip velocity phenomenon which can not be ignored especially for the non-Newtonian models. N_1 is the velocity slip factor which can be presumed to proportion to $(1 - at)^{\frac{1}{2}}$ for the similarity solution, so it can take the form $N_1 = N_0(1 - at)^{\frac{1}{2}}$, where N_0 is the initial value for the velocity slip factor ($N_1 = N_0$ at $t = 0$). Also, $h(t)$ is the uniform thickness of the thin elastic liquid film, which is located on the horizontal stretching sheet (Figure 1).

Non-dimensional transformations are normally offered as follows [27]:

$$\eta = \sqrt{\frac{b}{\nu(1 - at)}}\,y, \quad \psi = \sqrt{\frac{\nu b}{(1 - at)}}\,xf(\eta), \tag{8}$$

$$\begin{aligned} T &= T_0 - T_r\left(\frac{bx^2}{2\nu(1 - at)\sqrt{1 - at}}\right)\theta(\eta),\\ C &= C_0 - C_r\left(\frac{bx^2}{2\nu(1 - at)\sqrt{1 - at}}\right)\phi(\eta), \end{aligned} \tag{9}$$

where η is the non-dimensional variable, f is the dimensionless stream function, θ is the dimensionless temperature, and ϕ is the dimensionless concentration. It is interesting to note here that both the components of the fluid velocity u and v can be represented as the derivatives of the stream function ψ as follows:

$$u = \frac{\partial \psi}{\partial y}, \quad v = -\frac{\partial \psi}{\partial x}. \tag{10}$$

Applying the previous non-dimensional transformations help us to reach the following governing ordinary differential equations:

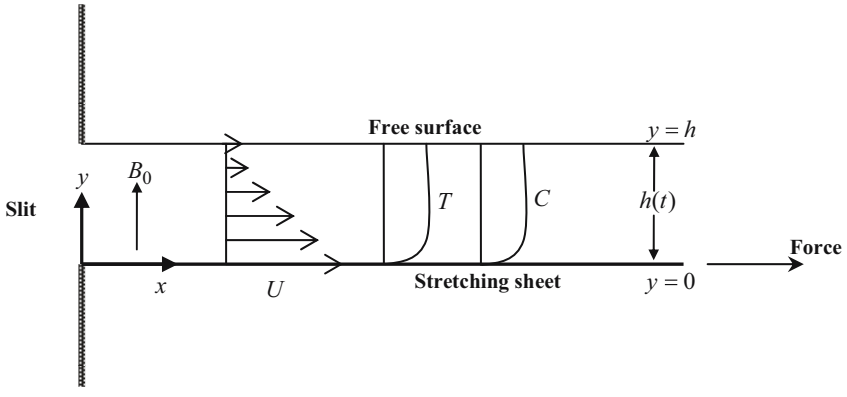

Figure 1: Physical configuration.

$$\left(1+\frac{1}{\beta}\right)f''' + ff'' - f'^2 - S\left(\frac{\eta}{2}f'' + f'\right) - Mf' = 0, \quad (11)$$

$$\left(\frac{1+R}{\mathrm{Pr}}\right)\theta'' + f\theta' - 2f'\theta - \frac{S}{2}(3\theta + \eta\theta') + \mathrm{Ec}\left(1+\frac{1}{\beta}\right)f''^2 + \mathrm{Nt}\theta'^2 + \mathrm{Nb}\theta'\phi' + M\mathrm{Ec}f'^2 = 0, \quad (12)$$

$$\frac{1}{\mathrm{Sc}}\phi'' + f\phi' - 2f'\phi - \frac{S}{2}(3\phi + \eta\phi') + \frac{\mathrm{Nt}}{\mathrm{ScNb}}\theta'' = 0, \quad (13)$$

together with the following associated boundary conditions [27]:

$$f(0) = 0,\ f'(0) = 1 + \lambda\left(1+\frac{1}{\beta}\right)f'',\ \theta(0) = 1,\ \phi(0) = 1, \quad (14)$$

$$f(\gamma) = \frac{\gamma}{2}S,\ f''(\gamma) = 0,\ \theta'(\gamma) = 0,\ \phi'(\gamma) = 0. \quad (15)$$

Now, we observe that the momentum equation (11) contains three parameters, β which is previously defined as a Casson parameter, $S = \frac{a}{b}$ which is defined as the unsteadiness parameter, and $M = \frac{\sigma B_0^2}{\rho b}$ which represents the magnetic number. On the other hand, in the energy equation there are five basic parameters, the radiation parameter $R = \frac{16\sigma^* T_0^3}{3k^*\kappa}$, the Prandtl number $\mathrm{Pr} = \frac{\nu}{\alpha}$, the Eckert number $\mathrm{Ec} = \frac{U^2}{c_p(T_w - T_0)}$, the thermophoresis parameter $\mathrm{Nt} = \frac{\tau D_T(T_w - T_0)}{\nu T_0}$, and the Brownian motion parameter $\mathrm{Nb} = \frac{\tau D_B(C_w - C_0)}{\nu}$. Furthermore, the remaining parameters can be defined as the Schmidt number $\mathrm{Sc} = \frac{\nu}{D_B}$, the slip velocity parameter $\lambda = N_0\sqrt{\frac{b}{\nu}}$, and the dimensionless film thickness γ. Additionally, the value of the film thickness γ can be calculated *via* equation (8) as follows:

$$\gamma = \left(\frac{b}{\nu(1-at)}\right)^{\frac{1}{2}}h. \quad (16)$$

Now, our main aim is to determine the unknown γ. Through the flow of fluid in the thin film layer, the film thickness varies with time and it can be easily obtained after differentiating the previous equation with respect to t, to give:

$$\frac{\mathrm{d}h}{\mathrm{d}t} = -\frac{a\gamma}{2}\left(\frac{\nu}{b(1-at)}\right)^{\frac{1}{2}}. \quad (17)$$

Three important physical quantities, the local skin-friction coefficient Cf_x, the wall temperature gradient Nu_x, and the wall concentration gradient Sh_x, are given by

$$\mathrm{Cf}_x\mathrm{Re}^{\frac{1}{2}} = -\left(1+\frac{1}{\beta}\right)f''(0),$$
$$\mathrm{Nu}_x\mathrm{Re}^{\frac{-1}{2}} = -\theta'(0),\ \mathrm{Sh}_x\mathrm{Re}^{\frac{-1}{2}} = -\phi'(0), \quad (18)$$

where $f''(0)$, $\theta'(0)$, and $\phi'(0)$ are dimensionless shear stress, the temperature gradient at the stretching sheet, and the concentration gradient at the stretching sheet, respectively. Also, $\mathrm{Re} = \frac{U_w x}{\nu}$ which appears in the last equation is the local Reynolds number.

3 Results and discussion

The obtained systems of equations which appear in equations (11)–(13) are non-linear, coupled, ordinary differential equations, which have no exact (analytical) solution. So, they ought to solve numerically together with the physical boundary condition equations (14)–(15). The shooting method discussed by Conte and de Boor [30] has been confirmed to be efficient and appropriate for the solution of these kinds of equations. So, because of the accuracy of the shooting method, it is employed in this article. Prior to investigating nanofluid flow and heat mass transfer techniques, the accuracy and validity of the obtained results, which resulted from employing the numerical shooting method, are first validated through the following comparison. The numerical data with previously published ones are introduced below in the following table for the thickness film γ and the skin-friction coefficient $-f''(0)$ for assorted values of S. Apparently, an excellent agreement is achieved. After that, results are obtained in Table 1 for various combinations of the physical parameters mentioned above. The curves in Figure 2 show that at lower unsteadiness parameter values S, larger dimensionless film thicknesses are obtained together with a diminishing for both the dimensionless velocity and the velocity values $f'(\gamma)$ at free surface. Also, the same figure clearly shows that the velocity of the non-Newtonian

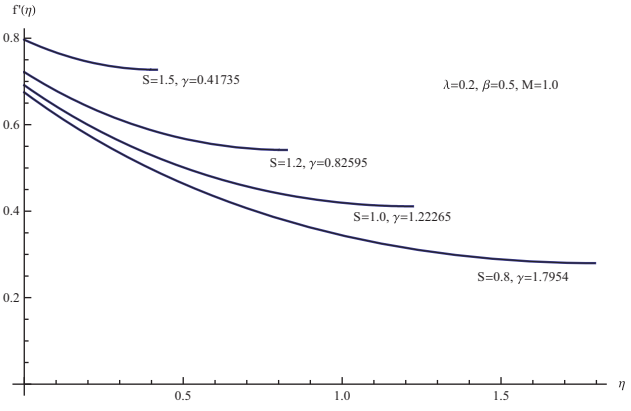

Figure 2: $f'(\eta)$ for assorted quantities of S.

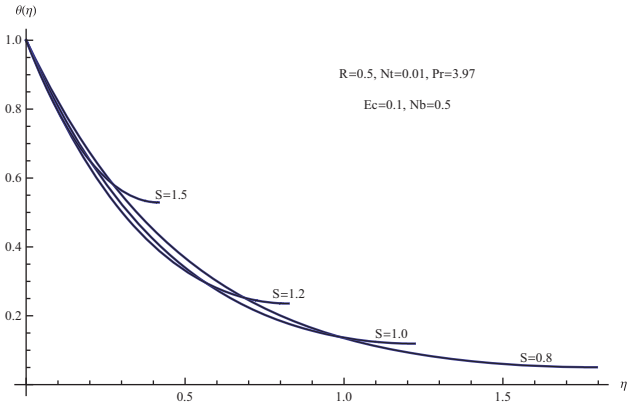

Figure 3: $\theta(\eta)$ for assorted quantities of S.

Table 1: Thickness film γ and the values of the drag force $-f''(0)$ for assorted value of S with $\beta \to \infty$ and $M = \lambda = 0$

S	Qasim *et al.* [27]		Present results	
	γ	$-\gamma f''(0)$	γ	$-\gamma f''(0)$
0.4	4.9814540	5.6494474	4.98145434	5.649439985
0.6	3.1317100	3.7427863	3.13170973	3.742785976
0.8	2.1519940	2.6809656	2.15199391	2.680964459
1.0	1.5436160	1.9723849	1.54361609	1.972384593
1.2	1.1277810	1.4426252	1.12777901	1.442624708
1.4	0.8210320	1.0127802	0.82103192	1.012779957

nanofluid over the sheet $f'(0)$ is an increasing function of unsteadiness parameter S, which physically means that nanofluid flow with great S grows faster than the flow with small S. It is also found that the dimensionless velocity $f'(\eta)$ through the liquid thin film layer enhances with augmenting the unsteadiness parameter. Likewise, at lower unsteadiness parameter values S, smaller temperature $\theta(y)$ at the ambient and smaller free surface concentration values $\phi(y)$ are obtained as observed in Figures 3 and 4, respectively. Indeed, the nanofluid concentration chooses the high values of unsteadiness parameter to pass to its improvement.

The velocity profiles as elucidated in Figure 5 indicate that the film thicknesses are larger for the minimal values of magnetic number M in the thin film layer. Also, the same behavior is observed for the fluid velocity along the sheet $f'(0)$.

Variations of temperature $\theta(\eta)$ as a function of η and concentration profiles $\phi(\eta)$ for assorted values of the same magnetic number M are introduced in Figures 6 and 7, respectively. It is motivating to observe that, a boost in the value of M is a reason for the enhancement of the distribution of temperature, the concentration distribution, the temperature $\theta(y)$ at the free surface, and the free surface concentration $\phi(y)$. After carefully having studied the effects of magnetic parameter on the temperature field, it could be observed that the magnetic parameter seems to act as a heating factor in the nanofluid flow.

Figure 8 shows the physical model predictions for the thickness of the liquid film and the dimensionless velocity distribution through the thin film region according to the variation in β. It is evident that the Newtonian fluid considerations ($\beta \to \infty$) have a more worthy impact on the film thickness in which the thickness becomes minimum when the fluid is closer to the Newtonian type ($\beta \to \infty$). Additionally, a paramount feature of the present results in the same figure is the prediction of both the velocity values $f'(y)$ at the free surface and the velocity of the non-Newtonian nanofluid along the sheet $f'(0)$ in which they reach the maximum as $\beta \to \infty$.

The increased Casson parameter β resulted in maximum temperature $\theta(y)$ at the free surface and extreme free surface concentration $\phi(y)$ as well as highly distribution for both temperature and concentration inside the

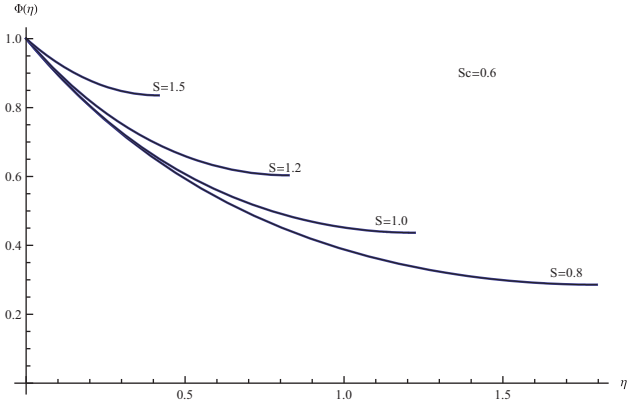

Figure 4: $\phi(\eta)$ for assorted quantities of S.

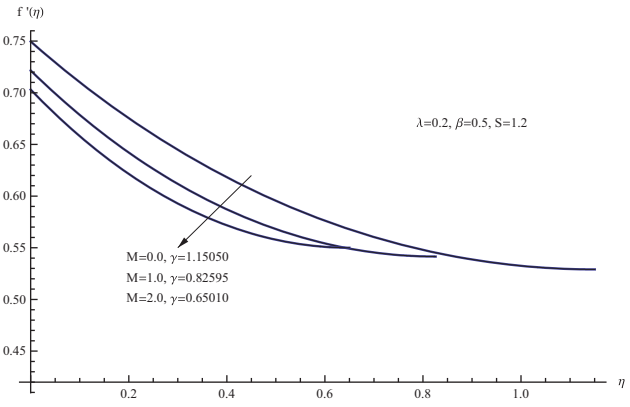

Figure 5: $f'(\eta)$ for assorted quantities of M.

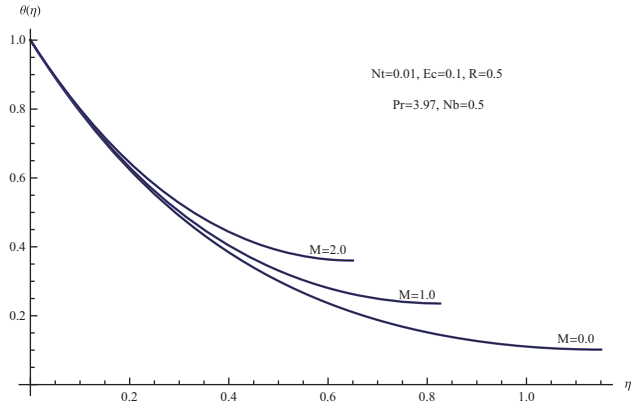

Figure 6: $\theta(\eta)$ for assorted quantities of M.

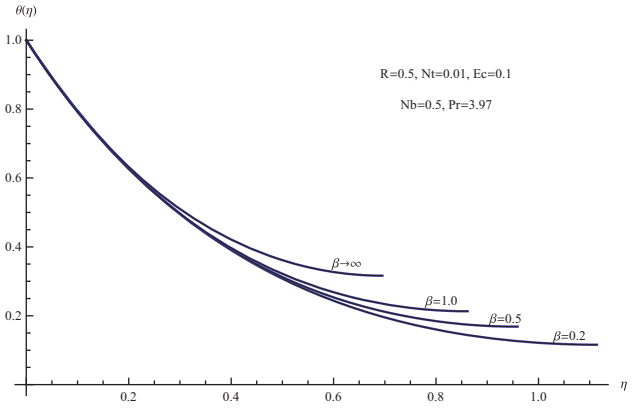

Figure 9: $\theta(\eta)$ for assorted quantities of β.

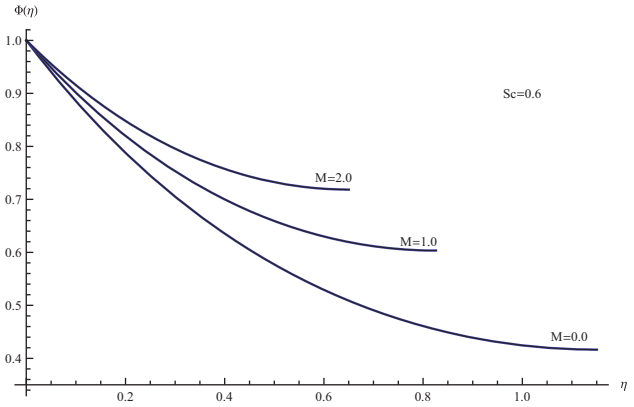

Figure 7: $\phi(\eta)$ for assorted quantities of M.

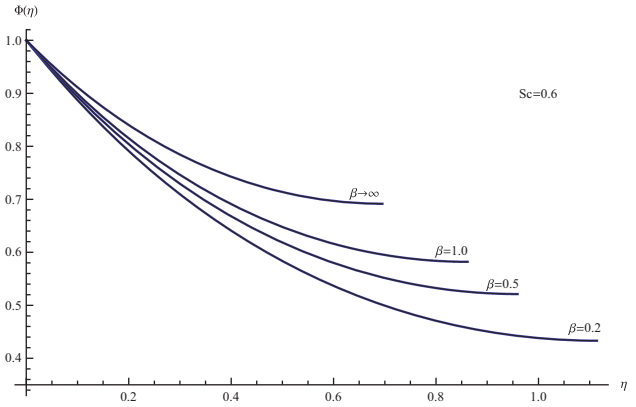

Figure 10: $\phi(\eta)$ for assorted quantities of β.

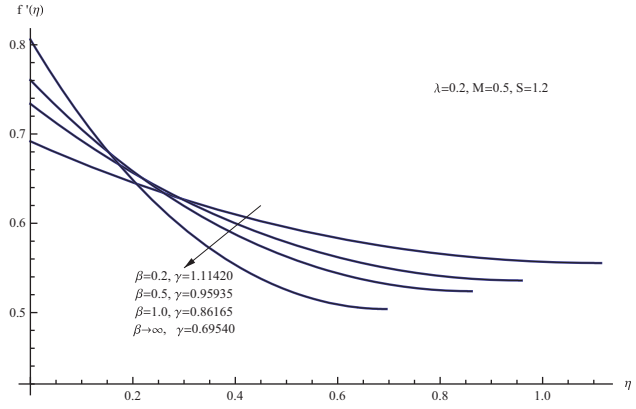

Figure 8: $f'(\eta)$ for assorted quantities of β.

liquid film layer as clearly observed in Figures 9 and 10. Physically, the Casson parameter should be sufficiently small, to achieve a satisfactory nanofluid cooling which is very much required, especially in some of the important technological applications.

Figure 11 depicts that by enhancing the values of the slip velocity parameter λ, both the velocity $f'(\eta)$ inside thin film layer and the film thickness γ decreases, while the completely contrary behavior is observed for the velocity values $f'(\gamma)$ at the free surface.

The profiles of temperature $\theta(\eta)$ and the profiles of concentration $\phi(\eta)$ for various values of the slip velocity parameter λ are demonstrated in Figures 12 and 13, respectively. It is noted that both the temperature and the concentration of the fluid flow increase with the increasing trend in λ through the film layer. Besides, we observe that the slip velocity parameter λ has considerable effects on both the temperature $\theta(\gamma)$ at the free surface and the free surface concentration $\phi(\gamma)$. When λ increases, both $\theta(\gamma)$ and $\phi(\gamma)$ enhance. Physically, within the film layer, both the nanofluid warming and the nanofluid concentration depend strongly on the great slip velocity parameter.

From Figure 14, it is clear that for big values of the parameter of radiation R, the temperature curve inside the thin film layer differs little from the small values of

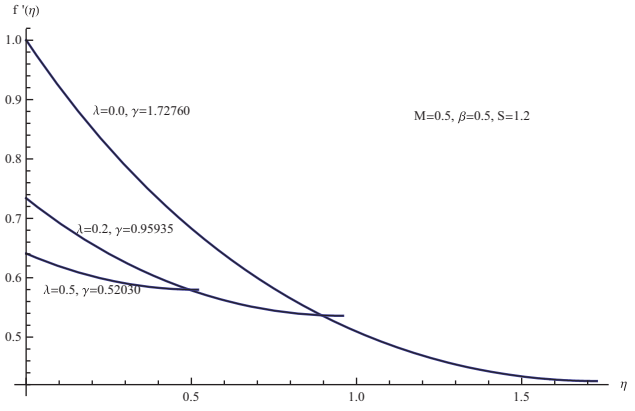

Figure 11: $f'(\eta)$ for assorted quantities of λ.

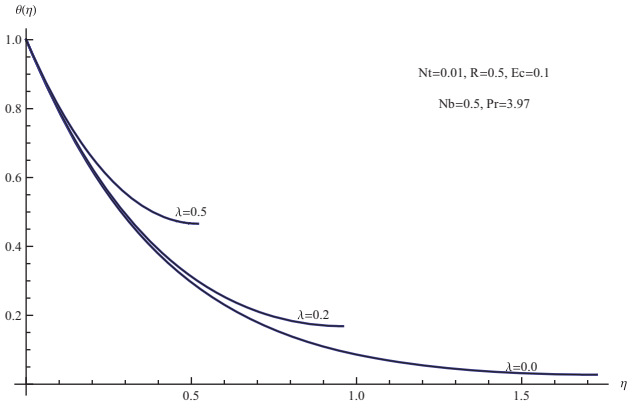

Figure 12: $\theta(\eta)$ for assorted quantities of λ.

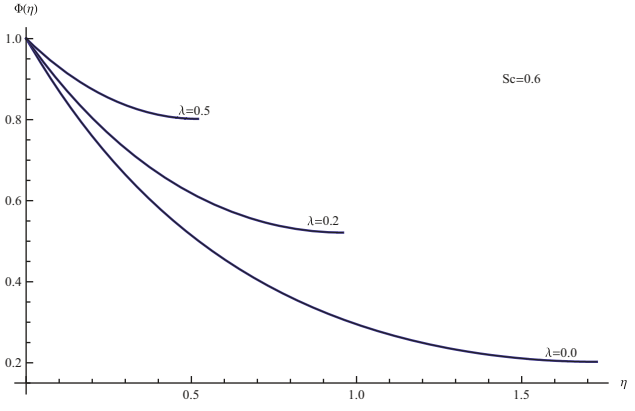

Figure 13: $\phi(\eta)$ for assorted quantities of λ.

R; however, when the parameter of radiation R enhances, these profiles show enhancement behavior for both the temperature throughout the film layer and the temperature $\theta(\gamma)$ at the free surface as well as a fixed thin film thickness. The physical interpretation for the following behavior is that the thermal radiation phenomenon can also be utilized to predict high warming rates of purely viscous nanofluids.

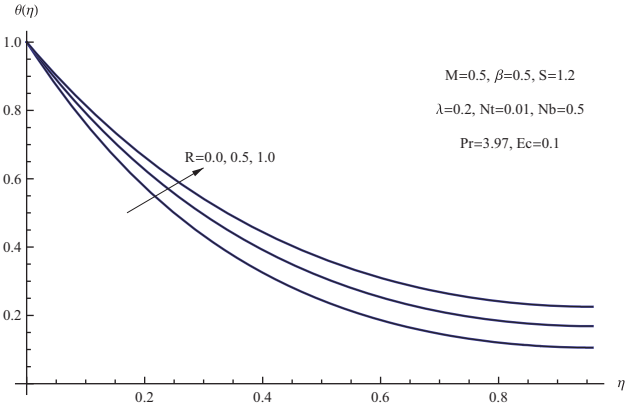

Figure 14: $\theta(\eta)$ for assorted quantities of R.

The impact of Eckert number Ec on the temperature curves is depicted in Figure 15. From these plots, we observe that the effect of viscous dissipation phenomenon results in promoting the thermal energy throughout the film layer as well as the temperature $\theta(\gamma)$ at the free surface. These observed results hold good for assorted values of the Eckert number. Clearly that, the Eckert number appears to act as a stimulating factor for warming the film region in which it has a very significant influence on the thermal film layer.

Temperature distributions $\theta(\eta)$ and concentration distributions $\phi(\eta)$ for various values of thermophoresis parameter Nt are shown in Figures 16 and 17, respectively. Clearly that a larger thermophoresis parameter results in a higher dimensionless free surface temperature $\theta(\gamma)$ and dimensionless free surface concentration $\phi(\gamma)$. In addition, $\theta(\eta)$ reaches its minimum value at Nt = 0.

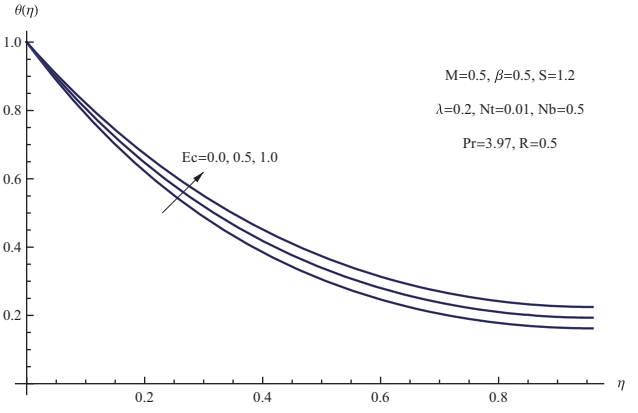

Figure 15: $\theta(\eta)$ for assorted quantities of Ec.

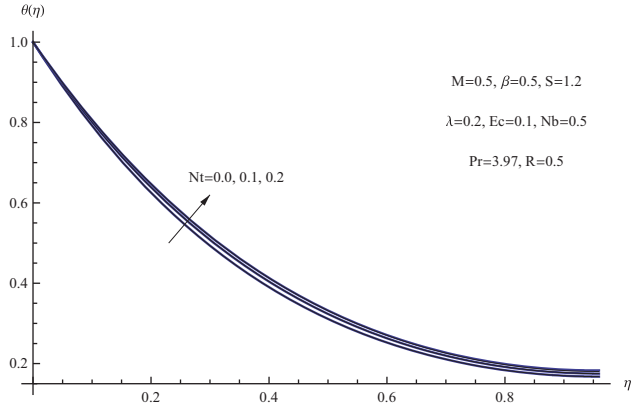

Figure 16: $\theta(\eta)$ for assorted quantities of Nt.

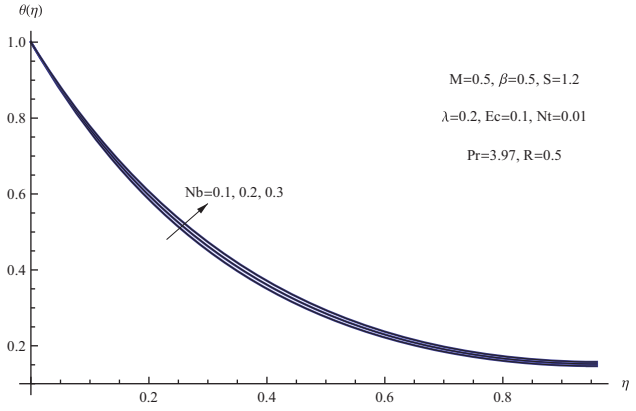

Figure 18: $\theta(\eta)$ for assorted quantities of Nb.

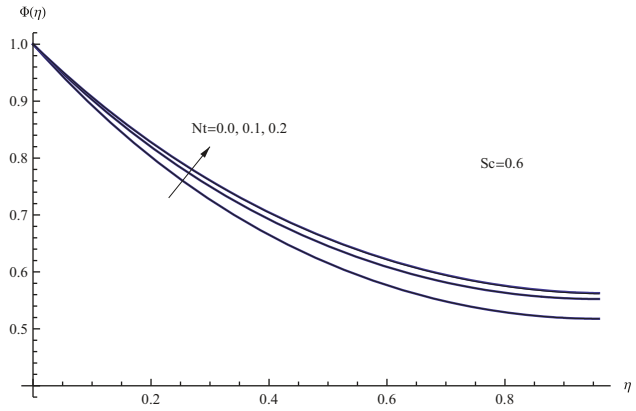

Figure 17: $\phi(\eta)$ for assorted quantities of Nt.

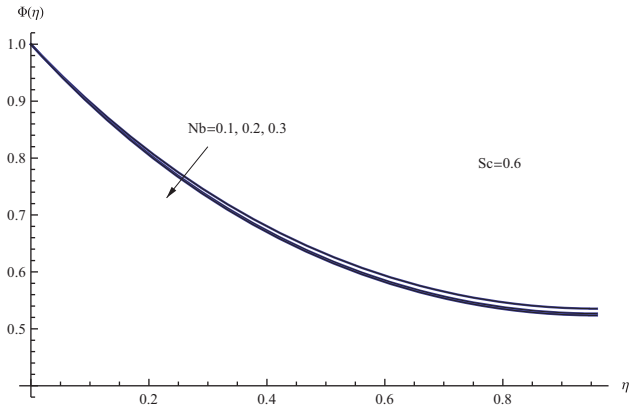

Figure 19: $\phi(\eta)$ for assorted quantities of Nb.

Figures 18 and 19 display, respectively, the variation of $\theta(\eta)$ and $\phi(\eta)$ with the Brownian parameter Nb. It is observed that at a given location η, $\theta(\eta)$ enhances with augment in the Brownian parameter Nb. Furthermore, it is clear from Figure 18 that the increasing Brownian parameter would reason the free surface temperature $\theta(\gamma)$ to enhance. Moreover, the impact of the same parameter on the dimensionless concentration $\phi(\eta)$ has quite opposite trend as illustrated in Figure 19.

Table 2 gives the values of $\mathrm{Cf}_x\mathrm{Re}^{\frac{1}{2}}$, $\mathrm{Nu}_x\mathrm{Re}^{\frac{-1}{2}}$, and $\mathrm{Sh}_x\mathrm{Re}^{\frac{-1}{2}}$, which represent, respectively, the values of skin-friction coefficient, the values of the local Nusselt number, and the values of the local Sherwood number, which is defined in equation (18) for several values of the governing parameters. Tabular data elucidate that the values of $\mathrm{Nu}_x\mathrm{Re}^{\frac{-1}{2}}$ decreased for all values of λ, R, Ec, Nt, and Nb. Thus, we find that there is a drastic change in the heat transfer characteristics of the Casson thin film flow when the aforementioned several effects are taken into account. Both the unsteadiness parameter S and Casson parameter β tend to decrease the values of $\mathrm{Cf}_x\mathrm{Re}^{\frac{1}{2}}$ and thereby also the local Sherwood number. Furthermore, the impact of magnetic number on $\mathrm{Cf}_x\mathrm{Re}^{\frac{1}{2}}$ is found to be more noticeable at large values, whereas a totally opposite trend is noted for the velocity slip parameter. Likewise, both the values of $\mathrm{Nu}_x\mathrm{Re}^{\frac{-1}{2}}$ and the values of $\mathrm{Sh}_x\mathrm{Re}^{\frac{-1}{2}}$ decrease when λ enhances. The cause of this physical behavior is that the thin film thickness becomes thin as the slip velocity parameter increases, which results in smaller values for both $\mathrm{Nu}_x\mathrm{Re}^{\frac{-1}{2}}$ and $\mathrm{Sh}_x\mathrm{Re}^{\frac{-1}{2}}$ at the surface. Finally, it is found that the local Sherwood number reduces with the growth of the magnetic number. However, it slightly increases with increase in both the radiation parameter and the Eckert number.

Table 2: Values for $Cf_x Re^{\frac{1}{2}}$, $Nu_x Re^{\frac{-1}{2}}$, and $Sh_x Re^{\frac{-1}{2}}$ for various values of S, M, β, λ, R, Ec, Nt, and Nb with Pr = 3.97 and Sc = 0.6

S	M	β	λ	R	Ec	Nt	Nb	$Cf_x(Re_x)^{\frac{1}{2}}$	$Nu_x Re^{\frac{-1}{2}}$	$Sh_x Re^{\frac{-1}{2}}$
0.8	1.0	0.5	0.2	0.5	0.1	0.01	0.5	1.626601	1.941910	1.116211
1.0	1.0	0.5	0.2	0.5	0.1	0.01	0.5	1.544731	2.105241	1.130440
1.2	1.0	0.5	0.2	0.5	0.1	0.01	0.5	1.392272	2.287381	1.077141
1.5	1.0	0.5	0.2	0.5	0.1	0.01	0.5	1.017640	2.405210	0.818659
1.2	0.0	0.5	0.2	0.5	0.1	0.01	0.5	1.252251	2.301941	1.238081
1.2	1.0	0.5	0.2	0.5	0.1	0.01	0.5	1.392272	2.287381	1.077141
1.2	2.0	0.5	0.2	0.5	0.1	0.01	0.5	1.484881	2.242960	0.935370
1.2	0.5	0.2	0.2	0.5	0.1	0.01	0.5	1.541242	2.260850	1.216691
1.2	0.5	0.5	0.2	0.5	0.1	0.01	0.5	1.330440	2.296791	1.156580
1.2	0.5	1.0	0.2	0.5	0.1	0.01	0.5	1.197443	2.317281	1.103971
1.2	0.5	0.5	0.0	0.5	0.1	0.01	0.5	2.478701	2.340581	1.405230
1.2	0.5	0.5	0.2	0.5	0.1	0.01	0.5	1.330440	2.296791	1.156580
1.2	0.5	0.5	0.5	0.5	0.1	0.01	0.5	0.718359	2.225960	0.796689
1.2	0.5	0.5	0.2	0.0	0.1	0.01	0.5	1.330440	2.673711	1.154312
1.2	0.5	0.5	0.2	0.5	0.1	0.01	0.5	1.330440	2.296791	1.156580
1.2	0.5	0.5	0.2	1.0	0.1	0.01	0.5	1.330440	2.037012	1.158091
1.2	0.5	0.5	0.2	0.5	0.0	0.01	0.5	1.330440	2.335921	1.156342
1.2	0.5	0.5	0.2	0.5	0.5	0.01	0.5	1.330440	2.140260	1.157521
1.2	0.5	0.5	0.2	0.5	1.0	0.01	0.5	1.330440	1.944522	1.158710
1.2	0.5	0.5	0.2	0.5	0.1	0.0	0.5	1.330440	2.309911	1.168690
1.2	0.5	0.5	0.2	0.5	0.1	0.1	0.5	1.330440	2.185721	1.054761
1.2	0.5	0.5	0.2	0.5	0.1	0.2	0.5	1.330440	2.113840	1.002950
1.2	0.5	0.5	0.2	0.5	0.1	0.01	0.1	1.330440	2.700031	1.094920
1.2	0.5	0.5	0.2	0.5	0.1	0.01	0.2	1.330440	2.592491	1.133412
1.2	0.5	0.5	0.2	0.5	0.1	0.01	0.3	1.330440	2.489610	1.146401

4 Conclusion

The theoretical analysis presented in this work accounts for viscous dissipation, thermophoresis, and the slip velocity effects on the thin film flow and heat mass transfer along the film layer for non-Newtonian Casson fluid which exposed to thermal radiation and magnetic field. This analysis represents an improvement over previous studies. Although strictly no exact solution can be obtained for the constitutive equations used here, the numerical shooting method that is employed in the present analysis has been demonstrated to yield useful results. The numerical procedure *via* the shooting method is given so that estimations of the film thickness, skin friction coefficient, local Nusselt number, local Sherwood number, and the velocity profile can be conveniently carried out. Comparison of the film thickness and skin-friction coefficient for the Casson thin film flow considered indicates that the results obtained exhibit good accuracy. The numerical calculations *via* shooting method have shown that:

1) The unsteadiness parameter, magnetic parameter, slip velocity parameter, and the Casson parameter have a very significant influence on the development of the film thickness.
2) The magnetic parameter, the unsteadiness parameter, the slip velocity parameter, and the Casson parameter have very significant effects on decreasing the rate of mass transfer.
3) The radiation parameter, Brownian parameter, Eckert number, and thermophoresis parameter do have a significant effect on the results, but the magnitude of the effect appears to be directly linked to the rate of heat transfer.
4) As a future work, we can apply an analytic approach such as homotopy analysis method to obtain convergent series solutions, especially for the non-Newtonian nanofluid problems under different physical assumptions.

Acknowledgements: The authors are thankful to the reviewers for their useful suggestions and comments which improved the quality of this article.

Funding information: The authors state no funding involved.

Author contributions: All authors have accepted responsibility for the entire content of this manuscript and approved its submission.

Conflict of interest: The authors state no conflict of interest.

References

[1] Wang CY. Liquid film on an unsteady stretching surface. Quart Appl Math. 1990;48:601–10.

[2] Andersson HI, Aarseth JB, Braud N, Dandapat BS. Flow of a power-law fluid on an unsteady stretching surface. J Non-Newtonian Fluid Mech. 1996;62:1–8.

[3] Andersson HI, Aarseth JB, Dandapat BS. Heat transfer in a liquid film on an unsteady stretching surface. Int J Heat Mass Transfer. 2000;43:69–74.

[4] Chen CH. Heat transfer in a power-law Fluid film over a unsteady stretching sheet. Heat Mass Transfer. 2003;39:791–6.

[5] Dandapat BS, Santra B, Andersson HI. Thermocapillarity in a liquid film on an unsteady stretching surface. Int J Heat Mass Transfer. 2003;46:3009–15.

[6] Chen CH. Marangoni effects on forced convection of power-law liquids in a thin film over a stretching surface. Phys Lett A. 2007;370:51–7.

[7] Liu IC, Andersson HI. Heat transfer in a liquid film on an unsteady stretching sheet. Int J Therm Sci. 2008;47:766–72.

[8] Abel MS, Mahesha N, Tawade J. Heat transfer in a liquid film over an unsteady stretching surface with viscous dissipation in presence of external magnetic field. Appl Math Model. 2009;33:3430–41.

[9] Noor NFM, Abdulaziz O, Hashim I. MHD flow and heat transfer in a thin liquid film on an unsteady stretching sheet by the homotopy analysis method. Int J Numer Meth Fluids. 2010;63:357–73.

[10] Noor NFM, Hashim I. Thermocapillarity and magnetic field effects in a thin liquid film on an unsteady stretching surface. Int J Heat Mass Transfer. 2010;53:2044–51.

[11] Nandeppanavar MM, Vajravelu K, Abel MS, Ravi S, Jyoti, H. Heat transfer in a liquid film over an unsteady stretching sheet. Int J Heat Mass Transfer. 2012;55:1316–24.

[12] Liu IC, Megahed AM. Numerical study for the flow and heat transfer in a thin liquid film over an unsteady stretching sheet with variable fluid properties in the presence of thermal radiation. J Mech. 2012;28:291–7.

[13] Khader MM, Megahed AM. Numerical studies for flow and heat transfer of the Powell-Eyring fluid thin film over an unsteady stretching sheet with internal heat generation using the Chebyshev finite difference method. J Appl Mech Tech Phys. 2013;54:440–50.

[14] Hussain SM, Jamshed W, Kumar V, Kumar V, Sooppy Nisar K, Eid MR, et al. Computational analysis of thermal energy distribution of electromagnetic Casson nanofluid across stretched sheet: Shape factor effectiveness of solid-particles. Energy Reports. 2021;7:7460–77.

[15] Jamshed W, Devi SSU, Safdar R, Redouane F, Nisar KS, Eid MR. Comprehensive analysis on copper-iron (II, III)/oxide-engine oil Casson nanofluid flowing and thermal features in parabolic trough solar collector. J Taibah Univ Sci. 2021;15:619–36.

[16] Alotaibi H, Althubiti S, Eid MR, Mahny KL. Numerical treatment of MHD flow of Casson nanofluid via convectively heated nonlinear extending surface with viscous dissipation and suction/injection effects. Comput Mater Continua. 2021;66:229–45.

[17] Vasu V, Rama Krishna K, Kumar ACS. Analytical prediction of forced convective heat transfer of fluids embedded with nanostructured materials (nanofluids). Pramana J Phys. 2007;69:411–21.

[18] Kakaç S, Pramuanjaroenkij A. Review of convective heat transfer enhancement with nanofluids. Int J Heat Mass Transf. 2009;52:3187–96.

[19] Khan WA, Pop I. Boundary-layer flow of a nanofluid past a stretching sheet. Int J Heat Mass Transf. 2010;53:2477–83.

[20] Hamad MA, Pop I. Scaling transformations for boundary layer flow near the stagnation-point on a heated permeable stretching surface in a porous medium saturated with a nanofluid and heat generation/absorption effects. Transport Porous Media. 2011;87:25–39.

[21] Hamad MAA, Ferdows M. Similarity solution of boundary layer stagnation-point flow towards a heated porous stretching sheet saturated with a nanofluid with heat absorption/generation and suction/blowing: A Lie group analysis. Commun Nonlinear Sci Numer Simulat. 2012;17:132–40.

[22] Makinde OD, Khan WA, Khan ZH. Buoyancy effects on MHD stagnation point flow and heat transfer of a nanofluid past a convectively heated stretching/shrinking sheet. Int J Heat Mass Transf. 2013;62:526–33.

[23] Shamshuddin MD, Abderrahmane A, Koulali A, Eid MR, Shahzad F, Jamshed W. Thermal and solutal performance of Cu/CuO nanoparticles on a non-linear radially stretching surface with heat source/sink and varying chemical reaction effects. Int Commun Heat Mass Transf. 2021;129:105710.

[24] Amine BM, Redouane F, Mourad L, Jamshed W, Eid MR, Al-Kouz W. Magnetohydrodynamics natural convection of a triangular cavity involving Ag-MgO/water hybrid nanofluid and provided with rotating circular barrier and a quarter circular porous medium at its right-angled corner. Arabian J Sci Eng. 2021;46:12573–97.

[25] Jamshed W, Nasir NAAM, Mohamed Isa SSP, Safdar R, Shahzad F, Nisar KS, et al. Thermal growth in solar water pump using Prandtl-Eyring hybrid nanofluid: a solar energy application. Scientific Reports. 2021;11:18704.

[26] Jamshed W, Eid MR, Nisar KS, Nasir NAAM, Edacherian A, Saleel CA, et al. A numerical frame work of magnetically driven Powell-Eyring nanofluid using single phase model. Scientific Reports. 2021;11:16500.

[27] Qasim M, Khan ZH, Lopez RJ, Khan WA. Heat and mass transfer in nanofluid over an unsteady stretching sheet using Buongiorno's model. Eur Phys J Plus. 2016;131:1–16.

[28] Raptis A. Flow of a micropolar fluid past a continuously moving plate by the presence of radiation. Int J Heat Mass Transf. 1998;41:2865–6.

[29] Raptis A. Radiation and viscoelastic flow. Int Comm Heat Mass Transfer. 1999;26:889–95.

[30] Conte SD, De Boor C. Elementary numerical analysis: An algorithmic approach. New York: McGraw-Hill; 1972.